euspen's 16th International Conference & Exhibition, Nottingham, UK, May 2016
www.euspen.eu

Control model for an over-determined fluid dynamic planar drive

B. Denkena[1], D. Dahlmann[1], T. Schumacher[1]

[1]Institute of Production Engineering and Machine Tools (IFW), Leibniz Universität Hannover, An der Universität 2, 30823 Garbsen, Germany

schumacher@ifw.uni-hannover.de

Abstract
A compact planar drive for the use in small machine tools has been developed. It is based on a fluid dynamic drive principle which enables translational motion in x- and y-direction as well as unlimited rotations around the z-axis in any position. Thrust forces are generated by deflection of 12 individually controlled fluid jets on the slide's flow grids.
This paper presents a three-layer control system for the novel drive. The top-level motion control calculates decoupled drive forces and torque for the slide's three mechanical degrees of freedom (DOF). Since the drive is over-actuated with 12 control inputs for the three DOFs, a control allocation algorithm coordinates the redundant thrust forces. The bottom level features the valve control for every single jet. First experiments demonstrate the functionality and limitations of the control system.

Keywords: Fluid dynamic planar drive, control allocation, micro machining

1. Introduction

The trend towards miniaturisation can be observed in many industrial sectors. Smaller parts with increasing complexity set high demands for future production technology. The great size ratio between current machine tools and typical work pieces indicates significant potential for economical, ecological and technical improvements in micro machining [1]. To make use of this potential a compact planar drive for small machine tools was developed and implemented in a prototype positioning stage. This stage integrates the drive and guiding functionality of three conventional machine axes in a very compact design [2]. It consists of two main components, namely the moving slide and the stationary frame. The inner part of the slide is made of steel. It acts as counter face for a magnetically pre-stressed aerostatic bearing, which guides the slide frictionless in the plane of motion. 8 areas of flow grids with alternating orientation are arranged on the 3D-printed outer part of the slide (Figure 1).

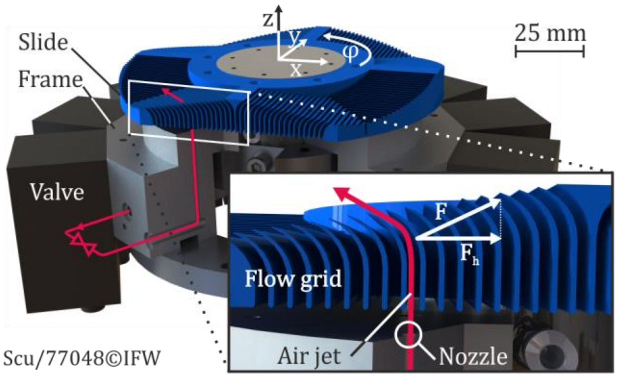

Figure 1. The fluid dynamic planar drive.

Table 1. Requirement specifications for the positioning stage.

Slide diameter	< 120 mm
Circular workspace (x- and y-direction)	> 20 mm
Rotations (φ)	∞
Static thrust force (x- and y- direction)	> 1 N

Each of the twelve nozzles, incorporated into the frame, forms an actuator with the opposing flow grid on the slide. Figure 1 shows an air jet streaming out of a nozzle, and being deflected on the flow grid. The horizontal component F_h of the resulting reaction force F drives the slide. Each air jet is controlled individually by a proportional valve. The position and orientation of the slide is detected by laser triangulation sensors as described in [2]. The requirement specifications for the fluid dynamic positioning stage are displayed in Table 1.

In the following, the overall controller design for the drive is introduced briefly. After that, the aspects of modeling and controlling the superposition of the redundant actuator forces are examined in detail. Finally the results of first function tests are presented.

2. Three Layer control-system

Motion control algorithms for over-actuated mechanical systems commonly include three hierarchical levels [3]. The top-level motion control of the fluid dynamic planar drive consists of three decoupled P + PI cascade controllers that were tuned experimentally. They compute a vector ${}_O\vec{u_c}$ of virtual control inputs to the three mechanical DOFs of the slide. It is given in the inertial coordinate frame O (see Figure 2) and contains two forces in the x- and y-direction as well as one moment around the z-axis. In the next step, a control allocation algorithm coordinates the 12 actuators to produce the desired virtual input torque and forces. This algorithm can be derived by inverting the static mechanical model of the drive, as shown in the following sections. On the lowest level, the force of each actuator is controlled individually. The proportional valves feature an integrated feedback control of the output pressure. The static relationship between valve output pressure and thrust force was integrated as a look-up table.

2.1 Static mechanical model

The application point of each actuator force depends on the position of the slide relative to the frame. The direction of force is opposite to the direction of jet deflection, and therefore also depends on the orientation of the flow grid. Since the flow grids are arranged at different angles, the grid sector (Figure 2) - each nozzle is directed on – has to be identified. This is done in the slide coordinate frame S by evaluating the polar angle of the nozzle position. Thus, the direction of force and its lever arm in respect to the slide's center of gravity M can easily be assigned to each actuator. The vector ${}_{S}\vec{u}$ contains the resulting drive forces in the $\tilde{x}$- and $\tilde{y}$-direction of the S-frame as well as the torque around the z-axis. It can be calculated for a given combination of actuator force magnitudes $\overrightarrow{u_a}$ by:

$${}_{S}\vec{u} = A(x, y, \varphi) \cdot \overrightarrow{u_a}$$

Wherein A is a 3 x 12 matrix that contains the unit vectors ${}_{(S)}\overrightarrow{d_{a,n}}$ in the direction of the actuator forces (Figure 2) and their associated levers.

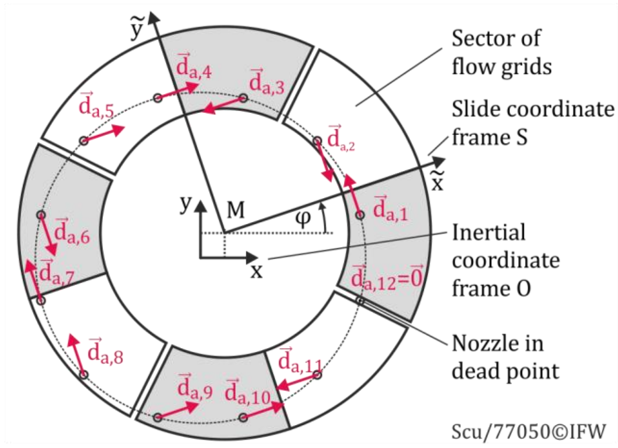

Figure 2. Nozzle positions and directions of the actuator forces.

2.2 Control allocation

The control allocation algorithm has to map the virtual control input from the top-level motion controllers to the 12 actuators such that the superimposed actuator forces and moments equal the command:

$$A(x, y, \varphi) \cdot \overrightarrow{u_a} \stackrel{!}{=} {}_{S}\overrightarrow{u_c} = {}^{S}T_{O}(x, y, \varphi) \cdot {}_{O}\overrightarrow{u_c}$$

In this equation, $\overrightarrow{u_a}$ is unknown and ${}^{S}T_{O}$ is the homogenous transform from O- to S-coordinate frame.

Since the mechanical system is over-actuated, the inverse problem - of solving the mechanical model for $\overrightarrow{u_a}$ - has no unique solution. Furthermore, the unidirectional working principle of the actuators constrains the solution space to vectors with positive entries. To meet these boundary conditions, an algorithm of 5 steps was derived and has to be run at every control cycle:

1. The virtual control inputs and nozzle positions are transformed to the S-coordinate frame.
2. The matrix A is set up by assigning force directions and calculating lever lengths for the actuators.
3. The Moore-Penrose pseudo-inverse A^{+} of A is calculated. This leads to the minimum magnitude solution $\overrightarrow{u_{a,min}}$.

$$\overrightarrow{u_{a,min}} = A^{+}(x, y, \varphi) \cdot {}_{S}\overrightarrow{u_v} = A^{T}(AA^{T})^{-1} \cdot {}_{S}\overrightarrow{u_v}$$

4. Actuators with negative control inputs are identified from the unrestrained solution $\overrightarrow{u_{a,min}}$. The mechanical system is then reduced by these actuators.
5. The minimum magnitude solution for the constrained allocation task is determined by calculating the pseudo inverse for the reduced system.

3. Results

The slide can be positioned within the circular workspace of 20 mm diameter. The unrestrained rotational capability of the drive has been proved for the whole workspace using laser triangulation sensors as described in [2]. These sensors run at a sample rate of 5 kHz and provide a linearity of 7.2 µm.

The standard deviation of the static positioning noise is 2.7 µm in x- and y-direction and 0.0086° in φ. It has to be taken into account that the standard deviation of the measurement noise is already 1.9 µm and 0.0078° respectively. Following a circular path with a diameter of 20 mm and a period time of 5 s resulted in a maximum tracking error of 0.188 mm. Fig 3 shows the results of the drive following a sinusoidal position signal in x-direction. At an amplitude of 10 mm and a period time of 5 s the maximum tracking error is 0.195 mm. Besides the tracking error, deviations in y and φ occur due to switching between different actuator combinations. The deviations in φ (Figure 3) are reproducible regardless of the sine frequency, if the integrator of the controller is deactivated. Therefore they cannot be explained by the control allocation itself or by the dynamic behavior of the valves. It is assumed that these errors result from local differences in the flow grids, which lead to position-dependent actuator characteristics.

With a slide mass of 0.393 kg and a maximum thrust force of 1 N the theoretical frequency limit for a sinusoidal path of 1 mm amplitude is 8 Hz. Experiments showed that the system follows a sweep reference signal up to 4.3 Hz. Higher frequencies lead to unstable behaviour.

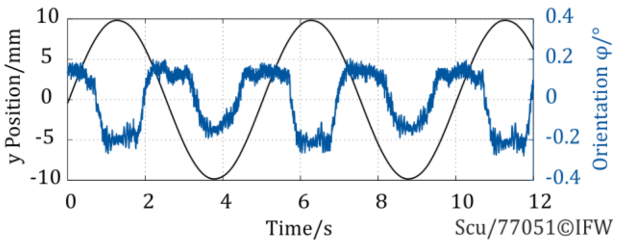

Figure 3. Effects of varying grid characteristics.

4. Summary and conclusion

This work introduces a control structure and a control allocation algorithm for the novel fluid dynamic planar drive. The experimental results confirm the functionality of the control allocation, and demonstrate the feasibility of the drive principle. It became apparent that the system lacks a deterministic actuator characteristic and cannot fulfill the precision requirements for micromachining yet. Future work has to focus on modelling the position dependencies of the actuators and on improving their dynamic behaviour.

Acknowledgement

The authors thank the German Research Foundation (DFG) for funding the presented work within the priority programme SPP1476 "Small machine tools for small work pieces".

References

[1] Wulfsberg, J. P.; Röhlig, B.: "Paradigm change: small machine tools for small workpieces". Production Engineering 7 (2013) 5, S. 465–468.

[2] Denkena, B.; Dahlmann, D.; Schumacher, T.: "Fluiddynamic Planar Drive with Unrestrained Rotational Degree of Freedom". Procedia CIRP 37 (2015), S. 71–76.

[3] Johansen, T. A.; Fossen, T. I.: "Control allocation—A survey". Automatica 49 (2013) 5, S. 1087–1103.